p16 Expression Represses DNA Damage Repair via a Novel Ubiquitin-Dependent Signaling Cascade.

David Molkentine
The University of Pittsburgh/UPMC Hillman Cancer Center
Jessica M. Molkentine
The University of Pittsburgh/UPMC Hillman Cancer Center
Kathleen A. Bridges
The University of Texas MD Anderson Cancer Center
Aakash Sheth
Baylor College of Medcine
David R Valdecanas
The University of Texas MD Anderson Cancer Center
Rishi Bahri
University of Pittsburgh, UPMC Hillman Cancer Center
Andrew J. Hefner
The University of Pittsburgh/UPMC Hillman Cancer Center
Manish Kumar
The University of Texas MD Anderson Cancer Center
Liang Yang
The University of Texas MD Anderson Cancer Center
Mohamed Abdelhakiem
The University of Pittsburgh/UPMC Hillman Cancer Center
Phillip M. Pifer
The University of Pittsburgh/UPMC Hillman Cancer Center
Vlad C. Sandulache
Dan L Duncan Comprehensive Cancer Center, Baylor College of Medicine
Beth M. Beadle
Stanford University Medical Center, Stanford University
Howard D. Thames
The University of Texas MD Anderson Cancer Center
Kathryn A. Mason
Retired
Curtis R. Pickering
The University of Texas MD Anderson Cancer Center
Raymond E. Meyn

Deceased

Heath D. Skinner (skinnerh@upmc.edu)

The University of Pittsburgh/UPMC Hillman Cancer Center

Research Article

Keywords: p16, HUWE1, USP7, TRIP12, radiation, head and neck cancer

Posted Date: March 29th, 2021

DOI: https://doi.org/10.21203/rs.3.rs-130839/v2

Abstract

Squamous cell carcinoma driven by human papillomavirus (HPV) is more sensitive to DNA-damaging therapies, such as radiation, than its HPV-negative counterpart. Here we show that p16, the clinically utilized surrogate for HPV positivity, renders cells more sensitive to radiation via a ubiquitin-dependent signaling pathway, linking high levels of this protein to increased activity of the transcription factor SP1, increased HUWE1 transcription and degradation of ubiquitin-specific protease 7 (USP7). Activation of this pathway in HPV-positive disease leads to an absence of TRIP12, decreased DNA damage repair as well as improved clinical outcomes. Conversely, repression of this pathway in HPV-negative disease is druggable via USP7 inhibitors under clinical development, resulting in potentiation of radiation response. Our findings may lead to improved outcomes for patients with HPV-negative radioresistant tumors, while allowing decreased intensity of therapy for patients with HPV-positive tumors.

Summary

In this manuscript we detail a previously undiscovered pathway directly linking p16 to DNA damage repair and resistance to radiation via ubiquitin-mediated degradation that is active in HPV-positive tumors, clinically relevant and targetable.

Introduction

Human papillomavirus (HPV) infection drives the development of cervical, anal, penile and head and neck squamous cell carcinoma (HNSCC)(1–3). Worldwide an estimated 630,000 cancer cases annually are related to HPV, with a relatively recent and dramatic increase in HPV-related HNSCC over the past two decades(3–6). Analyses of patient outcomes following standard of care radiation and platinum-based chemotherapy to treat HNSCC reveal that patients with HPV-positive (+) tumors fare significantly better than those with HPV-negative (-) tumors(7, 8). Also, *in vitro*, HPV (+) tumor cell lines are more sensitive to ionizing radiation than HPV (-) lines(9–13). These findings suggest that there is an inherent molecular mechanism by which HPV infection confers sensitivity of tumor cells to genotoxic therapy through the DNA damage response (DDR) pathway(14).

It is recognized that the hallmark of an HPV infection is the expression of the protein p16INK4 (hereafter referred to as p16)(7, 15–17), a consequence of E7-dependent pRb inhibition and degradation. Indeed, this protein is used as a surrogate biomarker for HPV in clinical settings due to its robustness and ease of use(15). p16 regulates the cell cycle(18), cell response to DNA damage(19–21) and cellular senescence following genotoxic exposure(22). Although felt to be largely non-functional in HPV-positive cancers, we have found that overexpression of p16 can simulate HPV-dependent radiation sensitivity, suggesting that this phenomenon is at least partially dependent on the function of p16(12, 21). Yet, it remains unclear how p16 achieves this effect. Understanding the basis of p16's ability to modulate the radiosensitivity of HPV (+) HNSCC cells could lead to strategies to enhance the response of HPV (-) tumors as well as perform rational treatment deintensification, both of which are sorely needed.

Recently, we established that one mechanism by which p16 modulates the cell response to DNA damage relies on its control of TRIP12(12), a HECT domain ubiquitin E3 ligase. TRIP12 binds to and inhibits RNF168 – an E3 ligase RING finger protein – and thus prevents excessive spreading of 53BP1-specific DNA repair foci by controlling the extent of chromatin ubiquitination at the sites of DNA damage(23). Cells expressing p16 have significantly downregulated protein levels of TRIP12(12) and enlarged 53BP1 foci in response to radiation therapy(23). Thus, it appears that p16 leads to a decrease in TRIP12 protein levels that compromises DNA repair at sites of radiation-induced DNA damage, specifically the repair of DNA double strand breaks (DSBs) by homologous recombination (HRR). Considering these findings, we proposed that an inverse relationship between p16 and TRIP12 may at least partially explain the increased positive response of HPV (+) patients to radiotherapy. It is currently unclear how p16 might regulate TRIP12 nor is it known whether this pathway is important to the clinical response and outcome. To address these questions, we modulated p16 in HPV (+) and HPV (-) HNSCC cell lines and examined USP7, a putative binding partner of TRIP12. This protein was ubiquitinated and degraded in the presence of p16 leading to a repression of TRIP12 and enhanced *in vitro* and *in vivo* response to radiation. We next explored USP7 binding partners via immunoprecipitation (IP)/mass spectrography (MS) analysis, which identified HUWE1 and TRIM21 as E3 ubquitin ligases binding USP7 in all HPV (+) and HPV (-) cell lines tested, although only HUWE1 was found to regulate USP7 expression. We then explored the connection between p16 and HUWE1, finding that HUWE1 is a transcriptionally regulated – potentially via Sp1 – intermediary between p16 and USP7, with increased expression leading to USP7 ubiquitination and degradation. We next examined HNSCC clinical samples from close to 400 patients, finding that HUWE1 expression is higher in HPV (+) disease, and that low levels of HUWE1 expression were associated with worse clinical outcome. Finally, we utilized several USP7 inhibitors under clinical development to radiosensitize HPV (-) HNSCC, thus delineating a p16-HUWE1-USP7-TRIP12 pathway regulating the DNA damage response in HNSCC that is both targetable and clinically relevant.

Results

Radiosensitivity in HNSCCs correlates with TRIP12 and USP7 expression and is HPV-status dependent

To identify the mechanism of HPV-mediated radiosensitization, we utilized a panel of HNSCC HPV (+) and HPV (-) cell lines. We examined the surviving fraction after 2 Gy of irradiation (SF2) for our panel and found that the HPV (+) cell lines (UMSCC-47, UPCI:SCC152, UPCI:SCC154) were significantly more sensitive to radiation than the HPV (-) lines (Detroit562, UMSCC-1, HN5, FaDu, HN30, HN31; Supplemental Fig. 1A). As expected, the HPV (-) cell lines expressed negligible levels of p16, the surrogate marker of HPV infection (Supplemental Fig. 1B). In agreement with our recently published report (12), p16 protein levels were inversely correlated with TRIP12 protein levels (Supplemental Fig. 1B).

Because we previously demonstrated that p16 regulates TRIP12 in a posttranslational fashion (12), we examined the expression of deubiquitinase ubiquitin-specific protease 7 (USP7), which has been shown

to bind to TRIP12(24). The immunoblot of USP7 from our cell line panel demonstrated a USP7 protein expression pattern proportional to that of TRIP12 (Supplemental Fig. 1B). Additionally, densitometric analysis showed that both USP7 and TRIP12 protein expression was highly correlated with radioresistance (Supplemental Fig. 1C).

p16 inhibits USP7 levels by increasing its ubiquitination and degradation

To assess whether the correlation between USP7 protein levels and radioresistance was a direct consequence of p16 expression, we examined the impact of direct p16 modulation on USP7 levels. The protein levels of USP7 decreased following forced expression of p16 in HPV (-) HN5 and HN31 cells (Fig. 1A). Moreover, forced expression of p16 in a larger panel including both HPV (-) HNSCC and non-small cell lung carcinoma (NSCLC) cell lines led to a similar reduction in USP7 protein expression (Fig. 1B). These findings indicate that p16 can repress USP7 expression. Additionally, this panel included p53 wild-type H460 and HN30 cells, which is suggestive of a p53-independent mechanism across multiple cell types. The converse was observed when p16 expression was inhibited via CRISPR in HPV (+) UM-SCC-47 cells, with USP7 levels increasing following p16 KO (Fig. 1C), suggesting that p16 regulates USP7 expression.

Next, we sought to determine the mechanism by which p16 regulates USP7. We found that forced p16 expression in HPV (-) HN5, HN30 and HN31 cells had no effect on USP7 mRNA (Supplemental Fig. 2A) despite the reduction seen at the protein level (Fig. 1A & B); this led us to suspect that the USP7 decrease may occur through posttranslational modification. To test this hypothesis, we performed cycloheximide chase assays to determine the effect of p16 expression on the stability of USP7. The presence of p16 significantly destabilized USP7 protein in p53 mutant HN5 (Fig. 1D) and p53 wild-type HN30 (Supplemental Fig. 2B). To determine whether this destabilization occurred through ubiquitination of USP7, we assessed whether the addition of the proteasome inhibitor MG132 could rescue USP7 expression following forced expression of p16. We found that MG132 was able to partially rescue the p16-induced reduction in USP7 protein expression in all three lines tested (Fig. 1E & Supplemental Fig. 2C), which indicates that the destabilization of USP7 by p16 depends on ubiquitination of USP7. To confirm the role of ubiquitination in this process, HN5 cells were co-transfected with control or p16 and lenti-HA-ubiquitin expression vectors. Cells were then either immunoprecipitated (IP) with HA-tagged ubiquitin and immunoblotted for USP7 or the reverse (Fig. 1F), both of which showed an increase in ubiquitination of USP7 in the presence of p16 expression. Furthermore, immunoprecipitation showed that the ubiquitination of USP7 was K48-linked and not K63-linked (Fig. 1G). Given that K-48-linked ubiquitination is generally associated with degradation(25), this finding suggests that the p16-dependent ubiquitination indeed marks the USP7 protein for destabilization and degradation.

USP7 stabilizes TRIP12 through deubiquitination

To identify whether USP7 was linked to the observed repression of TRIP12 by p16, we first immunoprecipitated TRIP12 and immunoblotted for USP7 in HPV (-) HN5 cells as well as the reverse

confirming that USP7 indeed bound to TRIP12 (Fig. 2A). In addition, direct targeting of USP7 via shRNA resulted in significant depression of TRIP12 protein levels in HPV (-) HN5, HN30 and HN31 cells (Fig. 2B), while inhibition of TRIP12 had no effect on USP7 expression (Supplemental Fig. 3A). This indicates that USP7 likely stabilizes TRIP12 in this model and not the converse. The regulation of TRIP12 by USP7 was confirmed in HPV (+) UM-SCC-47 and SCC-154 cells, where forced expression of USP7 led to significant upregulation of TRIP12 (Fig. C), despite the presence of p16, suggesting that p16 regulates TRIP12 indirectly through USP7.

While inhibition of USP7 reduced TRIP12 protein expression, it did not reduce TRIP12 gene expression (Supplemental Fig. 3B), providing evidence that TRIP12 regulation occurs through posttranslational modification. Cycloheximide chase assays in p53 mutant HN5 and p53 wild-type HN30 cells both showed a reduced half-life of TRIP12 after USP7 knockdown (Fig. 2D-E), which supports a p53-independent mechanism of TRIP12 stabilization by USP7. Treatment with MG132 at least partially reversed the reduction in TRIP12 protein expression induced by USP7 knockout in HN5, HN30 and HN31 cells (Fig. 2F and Supplemental Fig. 3C), suggesting that USP7 stabilizes TRIP12 by deubiquitination. To confirm the mechanism of TRIP12 stabilization by USP7, we performed immunoprecipitation (IP) for TRIP12 and evaluated the HA-tagged ubiquitin via immunoblot. This experiment showed that forced expression of p16 caused an increased ubiquitination of TRIP12, which was nearly abolished upon co-expression with USP7 (Fig. 2G), confirming that TRIP12 was indeed stabilized through deubiquitination by USP7.

p16 inhibits USP7 leading to increased radiosensitivity

To verify the link between an p16-USP7-TRIP12 axis and radiation response, we examined the effects of USP7 modulation following radiation both *in vitro* and *in vivo*. To investigate *in vitro* effects, we inhibited USP7 and examined BRCA1 and cell death following radiation treatment. Knockdown of USP7 with shRNA sensitized HN5 cells to radiation (Fig. 3A) and reduced BRCA1 expression (Fig. 3B). Immunocytochemical analysis of HN5 cells showed that targeting USP7 decreased the formation of BRCA1 foci following radiation exposure, suggesting that in the absence of USP7, the repair of radiation-induced DNA damage was compromised (Fig. 3C). This reduction in BRCA1 foci seen after inhibition of USP7 caused the cells to progress into mitosis with unrepaired DNA damage leading to aberrant mitosis, including increased centrosomes and micronuclei per cell, markers of mitotic death (Fig. 3D-F).

To examine the role of USP7 in p16-mediated radiosensitization, we expressed only p16 as well as both p16 and USP7 in HN5 cells. Forced expression of p16 resulted in significantly enhanced radiosensitivity compared to the vector transfected controls (Fig. 3G), and marked the downregulation of USP7, TRIP12, and BRCA1 (Fig. 3H). Forced expression of both p16 and USP7, on the other hand, partially reversed p16-induced radiosensitization (Fig. 3G) and p16-induced downregulation of both TRIP12 and BRCA1 (Fig. 3H). These results demonstrate that loss of USP7 is a factor in conferring radiosensitivity in HPV (+) tumors.

To examine the effects on radioresistance of USP7 modulation *in vivo*, we performed a tumor growth delay assay using HPV (-) HN5 xenografts in nude mice. Prior to inoculation, the cells were either infected

with control shRNA or USP7 shRNA to mimic USP7 deficiency observed in HPV (+) tumors. The animals were treated with 4 Gy for 5 consecutive days, and tumor diameters were measured every two days. At the end of the study, tumors were excised and analyzed by western blot, which confirmed shRNA knockdown of USP7 and showed reduced BRCA1 expression consistent with our *in vitro* results (Supplemental Fig. 4). Moreover, we found that inhibition of USP7 led to radiosensitization of HN5 tumors (Fig. 3I), further supporting the hypothesis that targeting USP7 could be a viable radiosensitization strategy for HPV (-) head and neck tumors.

IP/MS identifies TRIM21 and HUWE1 as E3 ubiquitin ligases for USP7

To understand how p16 modulates USP7 ubiquitination, we first identified binding partners of USP7 via performed immunoprecipitation mass spectrometry (IP/MS; schema in Fig. 4A) with an IP for USP7 followed by identification of proteins bound to USP7 in 3 HPV (-)/p16 (-) cell lines (HN5, HN30 and HN31) and 3 HPV (+)/p16 (+) cell lines (SCC152, SCC154 and UMSCC47). We identified three E3 ubiquitin ligases, i.e., HUWE1, TRIM21 and RNF168, binding USP7 in all HPV (-) cell lines tested (Fig. 4B, left column). For two of the HPV (+) cell lines, i.e., SCC-152 and SCC-154, USP7 had to be overexpressed prior to IP/MS due to insufficient levels of endogenous USP7. The HPV (+) cell lines had a similar set of binding partners with HUWE1 and TRIM21 binding USP7 in all 3 cell lines (Fig. 4B). A reverse IP/MS, with an IP for HUWE1 confirmed its binding with USP7 in all cell types examined (Fig. 4C).

p16 represses USP7 via transcriptional activation of HUWE1

To determine which of the identified E3 ubiquitin ligases may be regulating USP7, we initially performed immunoblots for HUWE1, TRIM21, USP7, TRIP12 and p16 in all six cell lines. Basal expression of HUWE1 showed an inverse relationship to both USP7 and TRIP12 as well as correlated with p16/HPV positivity, suggesting that this E3 ubiquitin ligase could be limiting USP7 expression (Fig. 5A). Conversely, TRIM21 was less associated with USP7, TRIP12 or p16 expression.

To verify the E3 ligase or ligases regulating USP7, we examined the gene expression of HUWE1 and TRIM21 in the previously evaluated cell lines. We found that HUWE1 gene expression correlated with p16/HPV positivity, indicating that HUWE1 is likely transcriptionally regulated by p16 (Fig. 5B). However, the gene expression of TRIM21 was comparable to its basal protein expression levels and did not show the inverse correlation expected if it were regulated by p16 (Fig. 5C). To investigate the implied transcriptional regulation of HUWE1 by p16, we expressed p16 in HN5 cells, which led to an increase in both HUWE1 protein and mRNA levels (Fig. 5D-E). This finding confirms that p16 regulates HUWE1 at the transcriptional level. Conversely, inhibition of p16 in HPV (+)/p16 (+) SCC154 cells led to a decrease in HUWE1 gene expression (Fig. 5F).

To confirm the link between p16, HUWE1 and USP7, HN5 cells with forced expression of p16 were co-transfected with HUWE1, TRIM21, TRIP12 or USP7 siRNA. Immunoblotting showed that HUWE1

expression increased with forced p16 expression (Fig. 5G), while TRIM21 did not appear to be affected by p16 expression, again confirming that p16 regulates HUWE1 and not TRIM12. Most importantly, p16-induced downregulation of USP7 and TRIP12 was rescued by co-transfection of HUWE1 siRNA (Fig. 5G) or stable expression of HUWE1 shRNA (Fig. 5H), confirming HUWE1 as an E3 ligase for USP7 downstream of p16. Moreover, in SCC-154 HPV (+)/p16 (+) cells, inhibition of HUWE1 via siRNA led to an increase in USP7 protein levels (Fig. 5I), demonstrating the importance of HUWE1 in the repression of USP7 expression by p16 in HPV (+) HNSCC. Additionally, forced expression of p16 in HN5 cells led to ubiquitination of USP7, which was rescued by cotransfection with HUWE1 shRNA, thus confirming that p16 regulates USP7 through its ubiquitination by HUWE1 (Fig. 5J).

To understand how p16 controls HUWE1 transcription, we examined the HUWE1 promoter region, which contains binding sites for multiple enhancers and promoters, including specificity protein 1 (SP1). SP1 is a transcription factor and has been found to bind to p16, leading to increased transcriptional activity of the target gene but not total expression level(26). To determine whether SP1 is the mediator of p16-driven upregulation of HUWE1, we inhibited SP1 expression in either HPV (-) HN5 cells forced to express p16 (Fig. 5K) or HPV (+)/p16 (+) UM47 cells (Fig. 5L). In the HPV (-) cells, HUWE1 levels increased as expected upon p16 expression, but this increase was reversed by SP1 inhibition (Fig. 5K). Similarly, inhibition of SP1 in HPV (+)/p16 (+) cells led to a decrease in HUWE1 expression (Fig. 5L). Thus, our results suggest that SP1 transcriptional activity is potentially responsible for the p16-driven HUWE1 upregulation.

Decreased HUWE1 expression is associated with worse disease-free survival in HPV (-) HNSCC

To determine if HUWE1 is associated with outcome in HNSCC, we examined both HUWE1 mutation and expression levels in the The Cancer Genome Atlas (TCGA) HNSCC patient cohort and evaluated their disease-free survival (DFS). We found that HUWE1 expression was elevated in HPV (+) tumors and markedly reduced in the small number of tumors with truncating HUWE1 mutations (Supplemental Fig. 5). In HPV (-) patients, low HUWE1 expression as a continuous variable was associated with worse DFS in univariate analysis ($p = 0.018$) and remained significant in multivariate analysis, including tumor site and clinical stage ($p = 0.016$). When divided into groups by HUWE1 expression (upper tertile (hi, blue line) vs. others (low, red line)), lower HUWE1 expression was associated with worse DFS ($p = 0.048$; Fig. 6A). Additionally, truncating mutations in HUWE1 led to a median DFS of 9.4 months compared to 67.7 months in the remaining patients ($p = 0.008$; Fig. 6C). Interestingly, in HPV (+) patients, neither HUWE1 mutation nor its gene expression was associated with survival (Fig. 6B & D). These data suggest that HUWE1 is present at high levels in clinical HPV (+) tumors, while its expression in HPV (-) HNSCC is repressed and associated with outcome and response to therapy.

USP7 is a druggable target to increase radiosensitivity

Because a p16-HUWE1-USP7-TRIP12 axis is associated with response to radiation and clinical outcome, we investigated whether USP7 is a druggable target to sensitize radioresistant tumors. Specifically, we modulated USP7 activity using three available USP7 inhibitors: GNE-6640, P22077 and P5091. GNE-6640

inhibits the deubiquitinase activity of USP7 with selectivity over a highly structurally similar deubiquitinase (USP47) and a highly active deubiquitinase (USP5)(27). P22077 and P5091 are less selective USP7 inhibitors, also inhibiting USP10 and USP47(28, 29).

Modulating USP7 activity via the chemical inhibitor GNE-6640 resulted in decreased TRIP12 expression (Fig. 7A-B) and increased radiosensitivity in HPV (-) HN5 cells (Fig. 7C). However, TRIP12 expression was only reduced with more than 6 hours of treatment (Fig. 7A) and at doses greater than 1 μM (Fig. 7B), which potentially explains the lack of radiosensitization seen at 1 or 10 μM with 6 hours of treatment prior to irradiation (Supplemental Fig. 6A) or at 1 μM with 48 hours of pretreatment (Fig. 7C). Similarly, BRCA1 foci were only reduced after treatment with 10 μM GNE-6640 for 48 hours prior to radiation (Fig. 7D) and not at any of the other doses or schedules tested (Supplemental Fig. 6B). This indicates that radiosensitization by GNE-6640 is only achieved when dose and duration are sufficient to reduce TRIP12 expression and BRCA1 foci formation. Similar radiosensitization was achieved using P5091 in HN5 and FaDu cells (Supplemental Fig. 6C-D) and P22077 in UMSCC25 and FaDu cells at various doses and schedules. These findings suggest that inhibiting USP7 could partially recapitulate HPV-induced radiosensitivity.

Discussion

HPV (-) tumors are more resistant to DNA-damage based therapies than their HPV (+) counterparts, particularly those arising in the head and neck. It is neither clear why this is the case, nor do any current therapies take advantage of intrinsic differences between the two tumor types to improve responses to DNA-damage based treatment. As resistance to this class of therapy – usually radiation in the setting of curative treatment – is the primary driver of death in most patients, translating insights from HPV (+) to HPV (-) tumors has significant potential to improve patient survival. Moreover, as radiation, especially in combination with chemotherapy, is a highly toxic therapy, biologically-driven radiosensitization could allow for decreased doses of radiation and better patient quality of life.

In this work, we present clear evidence that HPV-driven p16 expression represses TRIP12 and thus the repair of DNA damage via increased transcription of HUWE1 leading to ubiquitination and degradation of USP7. This is the first report of a direct signaling relationship between p16, HUWE1 and USP7, further elucidating the mechanism by which p16 inhibits DNA repair and the tumor cell response to DNA damage (see schematic pathway in Fig. 8). Moreover, we found that this pathway is both clinically important – as evidenced by the association between HUWE1 expression and patient outcome – and druggable via USP7 inhibitors, several of which are under evaluation for clinical use.

Despite being a clinical surrogate for HPV positivity(15), the function of p16 in HPV positive disease is far from clear. Classically, p16 is a tumor suppressor which inhibits cell cycle progression via suppression of CDK4/6 mediated phosphorylation of Rb. In most cellular contexts hypophosphorylated Rb binds to E2F family members leading to their sequestration. This prevents the expression of genes needed to enter S-phase, ultimately leading to cell cycle arrest and potentially cellular senescence(30). Indeed, in many

tumor types, repression of p16 expression – commonly via mutation or hypermethylation – is a key aspect of tumorigenesis, contributing to uncontrolled cell proliferation(31, 32). Conversely, in HPV (+) tumors, Rb is inactivated by E7, resulting in a release of negative feedback control on p16 expression and subsequent high levels(33). However, due to the inactivation of Rb in HPV (+) cells, p16 does not trigger cell cycle arrest in this context. Because of this loss of canonical p16 function, the high levels of p16 expression in HPV (+) disease is felt to be of less importance, aside from its utility as a clinical biomarker(15, 33).

This understanding belies the fact that p16 can have functions beyond its effects on Rb, CDK4/6 and cell cycle progression. For example, p16 can bind to and attenuate HIF-1α activity leading to decreased VEGF and tumor angiogenesis(34, 35), while loss of p16 is tumorigenic in the absence of Rb possibly via(36). Additionally, both our group and others have shown that inhibition of p16 can lead to potentiation of DNA-damage in a CDK4/6 independent fashion(12, 37), partially explaining the relative radiosensitivity of HPV (+) tumors. Our initial work examining this phenomenon led to the identification of TRIP12 repression by p16 leading to increased sensitivity to radiation in HPV (+) tumors, while high levels of TRIP12 expression in HPV (-) disease led to radioresistance.

Unfortunately, while TRIP12 can drive resistance to radiation, it is not yet targetable. This deficit combined with the lack of biologically-driven radiosensitizer currently available, drove us to identify additional upstream targets stabilizing TRIP12, with a goal of finding druggable drivers of radioresistance. By identifying p16-mediated repression of USP7 in HPV (+) cancer – leading to TRIP12 repression and sensitivity to radiation – we were able to use pharmacological inhibitors of USP7 to re-capitulate the radiosensitivity of HPV (+) cells in HPV (-) models. Our initial USP7 inhibitor, P5091, is not specific to USP7 but additionally inhibits USP47 (ubiquitin-specific peptidase 47), which, among several functions, controls tumor cell proliferation(38, 39). While P5091 is under clinical evaluation for multiple myeloma, it is unclear whether a USP7 or USP47-based mechanism is responsible for its antineoplastic activity. Thus, for clinical translation of our findings, it will be necessary to develop more specific inhibitors of USP7. To this end, we evaluated GNE-6640, a more specific inhibitor of USP7 deubiquitinase activity(27). Although not yet in clinical trials, our data support further exploration of GNE-6640 as a means of targeting USP7 to radiosensitize resistant head and neck tumors.

Our studies also identified HUWE1 as a direct link between p16 and USP7. HUWE1 is a HECT, UBA and WWE domain containing E3 ubiquitin protein ligase 1 that is involved in the stress response, proliferation, differentiation, apoptosis, and DNA repair(40). As an E3 ligase, HUWE1 marks proteins, including the DNA repair proteins BRCA1 and H2AX, with ubiquitin for degradation through the proteasome, thus decreasing the DNA repair capacity of both homologous recombination and nonhomologous end joining. Because HUWE1 and USP7 were also discovered to bind in our cell lines via IP/MS analysis, the E3 ubiquitin ligase HUWE1 may be antagonistic to USP7 and play an intermediary role in the p16/TRIP12 pathway and the inhibition of BRCA1 function. As we demonstrated in this report, knockdown of HUWE1 rescued p16-dependent downregulation of USP7 at the protein and gene levels, validating this prediction.

Finally, the E3 ligase HUWE1 was found to be transcriptionally controlled at least partially via SP1 downstream of p16, connecting p16 to USP7 protein expression (pathway in Fig. 8). Previously, it has been shown that p16 can form a complex with SP1, facilitating the transcriptional activity of the latter(26, 41). SP1 is one of several predicted transcription factors for HUWE1; however, our data are the first to our knowledge to show this regulation in any context, particularly in a p16-driven fashion.

Although our data do not rule out regulation of HUWE1 by p16 via other means, they do provide a direct link between p16 and HUWE1, rounding out a potentially complete pathway. Additionally, while we uncovered the roles of USP7 and HUWE1 in the p16-driven pathway responsible for regulating DNA damage through TRIP12, it is also possible that additional deubiquitinases control TRIP12 cellular levels and could act as intermediaries between p16 and TRIP12, leaving open possibilities for inherent or acquired therapeutic resistance.

In conclusion, we identified a signaling pathway directly connecting HPV positivity and p16 expression to ubiquitin-mediated DNA damage repair via transcriptional upregulation of HUWE1 followed by ubiquitin-dependent signaling to USP7 and TRIP12 (Fig. 8). This pathway is both clinically important – as evidenced by the relationship between HUWE1 and clinical outcome – and targetable via inhibitors of USP7. Identifying a novel, clinically relevant pathway mediating response to radiation both allows identification of patients who will respond well to treatment – to allow for decreased intensity of therapy – as well those patients who will be resistant to therapy and for whom targeting this pathway in combination with radiation may improve survival.

Materials And Methods

Cell Lines and Culture Conditions

Head and neck squamous cell carcinomas HN5, HN30, HN31, UM-SCC-1, UM-SCC-25 and UM-SCC-47 were obtained from Dr. Jeffrey Myers (UT MD Anderson). HEK-293T, FaDu, UPCI:SCC-152, UPCI:SCC-154, NCI-H460, NCI-H1299 and Detroit562 cells were purchased from ATCC. At every new frozen batch generation, DNA fingerprinting and mycoplasma testing were performed by the Cancer Center Support Grant-funded Characterized Cell Line core at MD Anderson (CA016672). HN5, HN30, HN31 and UM-SCC-1 cells were cultured in DMEM/F-12 (Mediatech) supplemented with 10% heat-inactivated (56°C, 30 min) FBS (Sigma) and 1% Pen-Strep (Gibco). NCI-H460 and NCI-H1299 cells were cultured in RPMI 1640 (Gibco) supplemented with 10% heat-inactivated FBS and 1% Pen-Strep. UM-SCC-47 cells were cultured in DMEM (Gibco) supplemented with 10% heat-inactivated FBS, 1% Pen-Strep, 2% MEM vitamins (Gibco), 1% sodium pyruvate (Lonza), and 1% nonessential amino acids (Gibco). FaDu, Detroit562, UPCI:SCC-152 and UPCI:SCC-154 were grown in MEM (Gibco) with 10% heat-inactivated FBS, 1% Pen-Strep and 1% sodium pyruvate. All cells were incubated at 37^{o}C, 5% carbon dioxide.

Clonogenic Survival Assays

Clonogenicity was tested following radiation using an X-RAD 320 biological irradiator (Precision X-Ray) as previously described*(12)*. Briefly, single cells were plated into 6-well dishes and incubated overnight. The next day, the cells were irradiated and then returned to the incubator for 10-21 days until colonies formed. Colonies with more than 50 cells were counted. Survival curves were generated by extrapolation from radiation surviving fractions using alpha/beta analysis with GraphPad Prism. Each experiment was plated in triplicate and repeated at least three independent times. Error bars represent standard error.

Antibodies and reagents

USP7, RNF168, ARF-BP1 (HUWE1) and TRIP12 antibodies were purchased from Abcam, p16 antibody from BD Biosciences, BRCA1, alpha tubulin and HA from Santa Cruz, K48 and K63-linked ubiquitin and Aurora Kinase A from Cell Signaling Technology, and Actin from Millipore. MG132 was purchased from Cell Signaling Technology, and cells were treated with doses ranging from 5-10 μM for 5-12 h. Cycloheximide was purchased from Sigma-Aldrich, and cells were treated with 300 μg/ml for the times indicated. GNE-6640 was purchased from Sigma-Aldrich, and cells were treated with doses ranging from 0.1 to 10 μM for 6 to 48 h prior to irradiation and left on until collection or staining of cells. P5091 was purchased from Sigma-Aldrich, and cells were treated with doses ranging from 1-5 μM for 1 h prior to and 18 h post irradiation.

Western blot analysis

Following treatment, cells were lysed with extraction buffer containing 20 mM HEPES (pH 7.9), 0.4 mM NaCl, 1 mM EDTA (pH 8.0), and 1 mM EGTA (pH 7.0). XPert protease and phosphatase inhibitors were added at a 1:100 dilution (GenDepot) and then sonicated. Equal amounts of protein were loaded into 4-15% gradient polyacrylamide gels (Bio-Rad) and then transferred to PVDF membranes for 10 min at 25 V using a Trans-Blot Turbo (Bio-Rad). Membranes were incubated in 5% dry milk for 1 h and then incubated with primary antibody overnight at 4°C. Immunoblots were detected using horseradish peroxidase-conjugated secondary antibodies (GE) and ECL2 chemiluminescent substrate (Pierce). Densitometry was measured using ImageJ. Western blots for TRIP12 were always run on the same day the cells were collected due to the instability of TRIP12 protein.

Over-expression and shRNA lentiviral infection

pLenti puro HA-Ubiquitin was a gift from Melina Fan (Addgene plasmid # 74218). Stable overexpression of USP7, p16 or rfp pLOC Turbo lentiviral vector (Precision LentiORF, Dharmacon) or stable shRNA knockdown of USP7 or p16 GIPZ lentiviral shRNA (Dharmacon) or GIPZ nonsilencial lentiviral shRNA control were cotransfected with lentiviral particles DR.8 and VSVG in HEK-293T cells for 48 h using Fugene (Promega) transfection reagent. Media plus lentivirus was then filtered through a 0.45-micron PES syringe filter and added to cells. Polybrene (5 μg/ml) was added, and the cells were transduced for 6 h. The transduction procedure was repeated for 2 consecutive days. Three days after initial transduction, stably expressing cells were selected with either 20 μg/ml blasticidin (overexpression) or 2 μg/ml puromycin (shRNA).

siRNA transfection

siRNA was transfected using Nucleofector II technology (Amaxa). Briefly, 1 million cells were resuspended in 100 µl Reagent T (Lonza) and 200 nM siRNA (Dharacon). Cells were electroporated with program T-001, plated in 6-well dishes containing complete media, and collected at the times indicated.

p16 CRISPR

A single colony of the LentiCRISPRv2 plasmid (Addgene) was expanded in LB broth containing 100 µg/ml ampicillin, and plasmid DNA was isolated using the QIAfilter Plasmid Midi Kit (Qiagen). The plasmid was then linearized and dephosphorylated by BsmBI digestion and purified with a QIAquick Gel Extraction Kit (Qiagen). p16 guide RNA, sgCDKN2A CACCGTTCGGCTGACTGGCTGGCCA, and reverse compliment, AAACTGGCCAGCCAGTCAGCCGAAC (Sigma), were annealed by PCR. gRNA was ligated into the purified LentiCRISPRv2 plasmid and transformed into One shot Stbl3 Chemically Competent *E. coli* (Invitrogen). A single clone was then selected, propagated, and Sanger sequenced to confirm the insert. The sg-p16 CRISPR plasmid was then cotransfected with DR.8 lentiviral particles and VSVG in HEK-293T cells for 48 h using Fugene (Promega) transfection reagent. Media containing lentivirus was then filtered through a 0.45-micron PES syringe filter and added to cells. Polybrene (5 µg/ml) was added, and the cells were transduced for 6 h. The transduction procedure was repeated for 2 consecutive days. Three days after initial transduction, stably expressing cells were selected with 2 µg/ml puromycin.

RT-PCR

Cells were collected and then lysed using a QIAshredder Kit (Qiagen). RNA extraction was performed using an RNeasy Kit (Qiagen), and RNA was quantified on a Take3 plate (BioTek) and read on an Epoch spectrophotometer (BioTek). Reverse transcription was performed using iScript Reverse Transcription Supermix (Bio-Rad) with 1 µg of total RNA/reaction. 50 ng of cDNA template was mixed with primers and SsoAdvanced Universal SYBR Green Supermix (BioRad). PrimePCR primer sets for GAPDH, HUWE1, TRIP12 or USP7 were purchased from BioRad. Real-time PCR was run on a CFX Connect Real-Time PCR system (BioRad). Data was normalized to GAPDH.

Immunocytochemistry

Cells were plated directly on a coverslip and allowed to adhere with overnight incubation. The following day, the cells were irradiated and fixed with 4% paraformaldehyde for 10 minutes at room temperature. Cells were then washed with PBS and permeabilized with 70% ethanol overnight at 4°C and for 20 minutes with 0.1% Igepal at room temperature. Cells were washed, blocked with 2% bovine serum albumin for 1 h and incubated overnight with 1:1000 Aurora Kinase A antibody (Cell Signaling Technology). Centrosomes were visualized by 1 h incubation with a 1:500 AlexaFluor 594 fluorochrome (Invitrogen). Cells were then incubated with 1:500 alpha tubulin (Santa Cruz) for 1 h at room temperature. Mitotic spindles were visualized by 1 h incubation with 1:600 FITC (Jackson Immuno), and pictures were captured with a Leica microscope. DNA was stained with 1 µg/ml DAPI (Sigma).

BRCA1 foci were visualized by incubating 1:500 BRCA1 antibody overnight (Santa Cruz) and 1:600 FITC (Jackson Immuno) for 45 minutes at room temperature.

Micronuclei quantification

HN5 cells stably expressing control or shUSP7 constructs were irradiated with 6 Gy and then incubated in medium containing 664 nM nocodazole (Sigma-Aldrich) for 4 h. At the end of nocodazole treatment, mitotic cells were harvested by gentle shaking and replated on coverslips in media without nocodazole for 24 h. Cells were then fixed and stained as described above.

Immunoprecipitation

Following treatment, cells were lysed with extraction buffer containing 20 mM Tris-HCl (pH 7.8), 150 mM NaCl, 1 mM EDTA (pH 8.0), and 1 mM EGTA (pH 7.0). XPert protease and phosphatase inhibitors were added at a 1:100 dilution (GenDepot) and then sonicated. 1 mg of cell lysate per sample was incubated with 5 µg of antibody of interest with rotation at 4°C overnight. Then, 30 µL of 100 mg/ml Protein-A Sepharose beads (GE Healthcare) were added to each sample and rotated at 4°C for 2 h. The beads were sedimented by centrifugation at 400 rcf, and the bead-bound samples were washed three times with 1 ml lysis buffer. The sample was eluted by heating the bead-bound sample with 25 µL 2X SDS Laemmli Sample Buffer (Bio-Rad) at 100°C for 7 min. After centrifugation, each sample was loaded into a 4-15% gradient polyacrylamide precast gel (Bio-Rad) and transferred to a PVDF membrane. The resulting sample was analyzed by immunoblot. Immunoprecipitations for TRIP12 were always run on the same day the cells were collected due to the instability of TRIP12 protein.

IP Mass Spectrometry

Following treatment, cells were lysed with extraction buffer containing 20 mM Tris-HCl (pH 7.8), 150 mM NaCl, 1 mM EDTA (pH 8.0), and 1 mM EGTA (pH 7.0). XPert protease and phosphatase inhibitors were added at a 1:100 dilution (GenDepot) and then sonicated. 25 mg of cell lysate per sample were incubated with 25 µg of antibody of interest with rotation at 4°C overnight. Then, 100 µL of 100 mg/ml Protein-A Sepharose beads (GE Healthcare) were added to each sample and rotated at 4°C for 2 h. The samples were sedimented by centrifugation, and the bead-bound samples were washed three times in lysis buffer. Beads were then sent to the MD Anderson Proteomics core for mass spectrometry analysis.

Xenograft Tumors

Mouse experiments were carried out in the specific pathogen-free mouse colony of the Department of Experimental Radiation Oncology at MD Anderson Cancer Center and were approved by the American Association for Accreditation of Laboratory Animal Care, in accordance with current regulations and standards of the U.S. Department of Agriculture and the Department of Health and Human Services. HN5 cells were transfected with USP7 shRNA using lentiviral vectors as described above. 2 million cells suspended in 20 µL PBS were injected intramuscularly into the right hind leg of male Swiss Nu/Nu mice. When tumors reached 8 mm in diameter (range 7.7-8.3 mm), the animals were randomized into groups

and treated with 4 Gy for 5 consecutive days using a 137 Cesium irradiator (dose rate 4 Gy/min). Mice were immobilized in a jig, and tumors were centered in a 3 cm diameter circular field for irradiation. The tumors were then measured every other day until they reached 14 mm in diameter. Animals were euthanized via CO_2 inhalation followed by cervical dislocation. Following euthanasia, the tumors were excised, and a portion of each was snap frozen and formalin fixed.

The time for tumors to reach 12 mm in diameter was used to determine the dose enhancement factor (DEF). The growth curves for the four conditions shown are approximately linear (coefficient of t^2 not significant for any of the curves), so the enhancement ratio for radiosensitization by USP7 was estimated as the ratio of growth delays between shUSP7 and controls. The calculations were carried out for three diameters (11, 12, and 13 mm) and either for all times or times > 6 days to assess the effect of small nonlinearities at the start. Because the observations were not independent (the same tumors are measured at different times), we applied so-called mixture models with random and fixed effects. Linear models where intercept and slope were considered random effects were used in a bootstrapping procedure where data were sampled randomly 100 times and estimates with 95% CIs were obtained from the 2.5- and 97.5-centile distributions. DEF at 11 mm shown in Figure 3, all calculated DEFs had a lower limit of the 95% CI greater than 1 by at least 0.5 arbitrary units.

Clinical data analysis

For expression analysis, HUWE1 mRNA expression was examined for all available patients from The Cancer Genome Atlas (TCGA) Head and Neck cohort for which HPV status was available (n=519). For outcome analysis, data for which HUWE1 mutation status and/or mRNA expression, HPV status and disease-free status were available (n=392). Clinical characteristics (see Supplemental Table 1), outcomes and biologic data were accessed via cBioPortal. Disease-free survival (DFS) was analyzed using Cox regression analysis. Kaplan-Meier survival curves are shown with log rank statistics used to compare groups for statistical significance.

Declarations

ACKNOWLEDGMENTS

IP/MS was performed with help from David Hawke at UT MD Anderson Cancer Center's Proteomics Facility funded in part by the NIH/NCI Cancer Center Support Grant (CCSG) #P30CA016672, the NIH High-End Instrumentation program grant #1S10OD012304-01, and CPRIT Core Facility Grant #RP130397.

Sanger sequencing was performed by the Advanced Technology Genomics Core at UT MD Anderson Cancer Center under NCI Grant CA016672 (ATGC).

This work was supported by i) the National Cancer Institute R01CA168485-08 (HS) and P50CA097190-15 (HS), ii) the National Institute for Dental and Craniofacial Research R01 DE028105 (HS) and R01DE028061 (HS and CP), and iii) The Cancer Prevention Institute of Texas RP150293 (HS and CP).

We thank Drs. Alma Faust and Anna Clemens for editorial assistance.

AUTHOR CONTRIBUTIONS

Conceptualization: DM, JM, RM, PP, CP, HS

Methodology: DM, JM, DV, KM, RM, VS, BB, HS

Investigation: DM, JM, KB, AS, RB, AH, MK, LY, DV, MA, HS

Visualization: JM, HS

Funding acquisition: HS, CP

Project administration: HS, CP, RM, KM

Supervision: KM, RM, HS

Writing – original draft: DM, JM, KB, HS

Writing – review & editing: DM, JM, KB, AS, RB, AH, MK, LY, BB, VS, MA, PP, DV, CP, HS

DECLARATION OF INTERESTS

The authors report no conflicts of interest related to this manuscript.

References

1. L. J. Viens, Human Papillomavirus–Associated Cancers — United States, 2008–2012, *MMWR Morb Mortal Wkly Rep* **65** (2016), doi:10.15585/mmwr.mm6526a1.
2. D. P. Zandberg, R. Bhargava, S. Badin, K. J. Cullen, The role of human papillomavirus in nongenital cancers, *CA: A Cancer Journal for Clinicians* **63**, 57–81 (2013).
3. M. Arbyn, S. de Sanjosé, M. Saraiya, M. Sideri, J. Palefsky, C. Lacey, M. Gillison, L. Bruni, G. Ronco, N. Wentzensen, J. Brotherton, Y.-L. Qiao, L. Denny, J. Bornstein, L. Abramowitz, A. Giuliano, M. Tommasino, J. Monsonego, EUROGIN 2011 roadmap on prevention and treatment of HPV-related disease, *Int J Cancer* **131**, 1969–1982 (2012).
4. C. de Martel, M. Plummer, J. Vignat, S. Franceschi, Worldwide burden of cancer attributable to HPV by site, country and HPV type: Worldwide burden of cancer attributable to HPV, *Int. J. Cancer* **141**, 664–670 (2017).
5. A. P. Stein, S. Saha, J. L. Kraninger, A. D. Swick, M. Yu, P. F. Lambertg, R. Kimple, Prevalence of human papillomavirus in oropharyngeal cancer: a systematic review, *Cancer J* **21**, 138–146 (2015).
6. V. Senkomago, S. J. Henley, C. C. Thomas, J. M. Mix, L. E. Markowitz, M. Saraiya, Human Papillomavirus-Attributable Cancers - United States, 2012–2016, *MMWR Morb Mortal Wkly Rep* **68**,

724–728 (2019).

7. K. K. Ang, J. Harris, R. Wheeler, R. Weber, D. I. Rosenthal, P. F. Nguyen-Tân, W. H. Westra, C. H. Chung, R. C. Jordan, C. Lu, H. Kim, R. Axelrod, C. C. Silverman, K. P. Redmond, M. L. Gillison, Human papillomavirus and survival of patients with oropharyngeal cancer, *N. Engl. J. Med.* **363**, 24–35 (2010).
8. M. L. Gillison, G. D'Souza, W. Westra, E. Sugar, W. Xiao, S. Begum, R. Viscidi, Distinct Risk Factor Profiles for Human Papillomavirus Type 16–Positive and Human Papillomavirus Type 16–Negative Head and Neck Cancers, *Journal of the National Cancer Institute* **100**, 407–420 (2008).
9. C. J. Busch, M. Kriegs, S. Laban, S. Tribius, R. Knecht, C. Petersen, E. Dikomey, T. Rieckmann, HPV-positive HNSCC cell lines but not primary human fibroblasts are radiosensitized by the inhibition of Chk1, *Radiotherapy and oncology: journal of the European Society for Therapeutic Radiology and Oncology* **108**, 495–9 (2013).
10. T. Rieckmann, S. Tribius, T. J. Grob, F. Meyer, C. J. Busch, C. Petersen, E. Dikomey, M. Kriegs, HNSCC cell lines positive for HPV and p16 possess higher cellular radiosensitivity due to an impaired DSB repair capacity, *Radiotherapy and oncology: journal of the European Society for Therapeutic Radiology and Oncology* **107**, 242–6 (2013).
11. J. M. Molkentine, D. P. Molkentine, K. A. Bridges, T. Xie, L. Yang, A. Sheth, T. P. Heffernan, D. A. Clump, A. Z. Faust, R. L. Ferris, J. N. Myers, M. J. Frederick, K. A. Mason, R. E. Meyn, C. R. Pickering, H. D. Skinner, Targeting DNA damage response in head and neck cancers through abrogation of cell cycle checkpoints, *Int. J. Radiat. Biol.*, 1–8 (2020).
12. L. Wang, P. Zhang, D. P. Molkentine, C. Chen, J. M. Molkentine, H. Piao, U. Raju, J. Zhang, D. R. Valdecanas, R. C. Tailor, H. D. Thames, T. A. Buchholz, J. Chen, L. Ma, K. A. Mason, K.-K. Ang, R. E. Meyn, H. D. Skinner, TRIP12 as a mediator of human papillomavirus/p16-related radiation enhancement effects, *Oncogene* **36**, 820–828 (2017).
13. R. J. Kimple, M. A. Smith, G. C. Blitzer, A. D. Torres, J. A. Martin, R. Z. Yang, C. R. Peet, L. D. Lorenz, K. P. Nickel, A. J. Klingelhutz, P. F. Lambert, P. M. Harari, Enhanced Radiation Sensitivity in HPV-Positive Head and Neck Cancer, *Cancer Res* **73**, 4791–4800 (2013).
14. H. Mirghani, F. Amen, Y. Tao, E. Deutsch, A. Levy, Increased radiosensitivity of HPV-positive head and neck cancers: Molecular basis and therapeutic perspectives, *Cancer Treat Rev* **41**, 844–852 (2015).
15. J. S. Lewis, B. Beadle, J. A. Bishop, R. D. Chernock, C. Colasacco, C. Lacchetti, J. T. Moncur, J. W. Rocco, M. R. Schwartz, R. R. Seethala, N. E. Thomas, W. H. Westra, W. C. Faquin, Human Papillomavirus Testing in Head and Neck Carcinomas: Guideline From the College of American Pathologists, *Arch Pathol Lab Med* **142**, 559–597 (2018).
16. J. P. Klussmann, E. Gultekin, S. J. Weissenborn, U. Wieland, V. Dries, H. P. Dienes, H. E. Eckel, H. J. Pfister, P. G. Fuchs, Expression of p16 protein identifies a distinct entity of tonsillar carcinomas associated with human papillomavirus, *The American journal of pathology* **162**, 747–53 (2003).
17. A. K. El-Naggar, W. H. Westra, p16 expression as a surrogate marker for HPV-related oropharyngeal carcinoma: a guide for interpretative relevance and consistency, *Head & neck* **34**, 459–61 (2012).

18. M. Hall, S. Bates, G. Peters, Evidence for different modes of action of cyclin-dependent kinase inhibitors: p15 and p16 bind to kinases, p21 and p27 bind to cyclins, *Oncogene* **11**, 1581–8 (1995).
19. Y. Matsumura, N. Yamagishi, J. Miyakoshi, S. Imamura, H. Takebe, Increase in radiation sensitivity of human malignant melanoma cells by expression of wild-type p16 gene, *Cancer letters* **115**, 91–6 (1997).
20. A. W. Lee, J. H. Li, W. Shi, A. Li, E. Ng, T. J. Liu, H. J. Klamut, F. F. Liu, p16 gene therapy: a potentially efficacious modality for nasopharyngeal carcinoma, *Molecular cancer therapeutics* **2**, 961–9 (2003).
21. S. Kawabe, J. A. Roth, D. R. Wilson, R. E. Meyn, Adenovirus-mediated p16INK4a gene expression radiosensitizes non-small cell lung cancer cells in a p53-dependent manner, *Oncogene* **19**, 5359–66 (2000).
22. R. Mirzayans, B. Andrais, G. Hansen, D. Murray, Role of p16(INK4A) in Replicative Senescence and DNA Damage-Induced Premature Senescence in p53-Deficient Human Cells, *Biochemistry research international* 2012, 951574 (2012).
23. T. Gudjonsson, M. Altmeyer, V. Savic, L. Toledo, C. Dinant, M. Grofte, J. Bartkova, M. Poulsen, Y. Oka, S. Bekker-Jensen, N. Mailand, B. Neumann, J. K. Heriche, R. Shearer, D. Saunders, J. Bartek, J. Lukas, C. Lukas, TRIP12 and UBR5 suppress spreading of chromatin ubiquitylation at damaged chromosomes, *Cell* **150**, 697–709 (2012).
24. X. Liu, X. Yang, Y. Li, S. Zhao, C. Li, P. Ma, B. Mao, Trip12 is an E3 ubiquitin ligase for USP7/HAUSP involved in the DNA damage response, *FEBS Letters* **590**, 4213–4222 (2016).
25. K. Ramadan, M. Meerang, Degradation-linked ubiquitin signal and proteasome are integral components of DNA double strand break repair: New perspectives for anti-cancer therapy, *FEBS Lett* **585**, 2868–2875 (2011).
26. H. H. Al-Khalaf, P. Mohideen, S. C. Nallar, D. V. Kalvakolanu, A. Aboussekhra, The cyclin-dependent kinase inhibitor p16INK4a physically interacts with transcription factor Sp1 and cyclin-dependent kinase 4 to transactivate microRNA-141 and microRNA-146b-5p spontaneously and in response to ultraviolet light-induced DNA damage, *J Biol Chem* **288**, 35511–35525 (2013).
27. L. Kategaya, P. Di Lello, L. Rougé, R. Pastor, K. R. Clark, J. Drummond, T. Kleinheinz, E. Lin, J.-P. Upton, S. Prakash, J. Heideker, M. McCleland, M. S. Ritorto, D. R. Alessi, M. Trost, T. W. Bainbridge, M. C. M. Kwok, T. P. Ma, Z. Stiffler, B. Brasher, Y. Tang, P. Jaishankar, B. R. Hearn, A. R. Renslo, M. R. Arkin, F. Cohen, K. Yu, F. Peale, F. Gnad, M. T. Chang, C. Klijn, E. Blackwood, S. E. Martin, W. F. Forrest, J. A. Ernst, C. Ndubaku, X. Wang, M. H. Beresini, V. Tsui, C. Schwerdtfeger, R. A. Blake, J. Murray, T. Maurer, I. E. Wertz, USP7 small-molecule inhibitors interfere with ubiquitin binding, *Nature* **550**, 534–538 (2017).
28. M. Altun, H. B. Kramer, L. I. Willems, J. L. McDermott, C. A. Leach, S. J. Goldenberg, K. G. S. Kumar, R. Konietzny, R. Fischer, E. Kogan, M. M. Mackeen, J. McGouran, S. V. Khoronenkova, J. L. Parsons, G. L. Dianov, B. Nicholson, B. M. Kessler, Activity-Based Chemical Proteomics Accelerates Inhibitor Development for Deubiquitylating Enzymes, *Chemistry & Biology* **18**, 1401–1412 (2011).

29. M. S. Ritorto, R. Ewan, A. B. Perez-Oliva, A. Knebel, S. J. Buhrlage, M. Wightman, S. M. Kelly, N. T. Wood, S. Virdee, N. S. Gray, N. A. Morrice, D. R. Alessi, M. Trost, Screening of DUB activity and specificity by MALDI-TOF mass spectrometry, *Nat Commun* **5**, 4763 (2014).
30. C. Romagosa, S. Simonetti, L. López-Vicente, A. Mazo, M. E. Lleonart, J. Castellvi, S. Ramon y Cajal, p16 Ink4a overexpression in cancer: a tumor suppressor gene associated with senescence and high-grade tumors, *Oncogene* **30**, 2087–2097 (2011).
31. G. Ciriello, M. L. Miller, B. A. Aksoy, Y. Senbabaoglu, N. Schultz, C. Sander, Emerging landscape of oncogenic signatures across human cancers, *Nature Genetics* **45**, 1127–1133 (2013).
32. A. Ko, S. Y. Han, and J. Song, Regulatory Network of ARF in Cancer Development, *Moleucles and Cells* **41**, 381–389 (2018).
33. C. H. Chung, M. L. Gillison, Human Papillomavirus in Head and Neck Cancer: Its Role in Pathogenesis and Clinical Implications, *Clin Cancer Res* **15**, 6758–6762 (2009).
34. J. Zhang, A. Lu, L. Li, J. Yue, Y. Lu, p16 Modulates VEGF Expression via Its Interaction With HIF-1α in Breast Cancer Cells, *Cancer investigation* **28**, 588 (2010).
35. P. Baruah, M. Lee, P. O. G. Wilson, T. Odutoye, P. Williamson, N. Hyde, J. C. Kaski, I. E. Dumitriu, Impact of p16 status on pro- and anti-angiogenesis factors in head and neck cancers, *British Journal of Cancer* **113**, 653 (2015).
36. M. Sen, N. Akeno, A. Reece, A. L. Miller, D. S. Simpson, K. A. Wikenheiser-Brokamp, p16 controls epithelial cell growth and suppresses carcinogenesis through mechanisms that do not require RB1 function, *Oncogenesis* **6**, e320–e320 (2017).
37. R. Dok, P. Kalev, E. J. V. Limbergen, L. A. Asbagh, I. Vázquez, E. Hauben, A. Sablina, S. Nuyts, p16INK4a Impairs Homologous Recombination–Mediated DNA Repair in Human Papillomavirus–Positive Head and Neck Tumors, *Cancer Res* **74**, 1739–1751 (2014).
38. S. Yan, Y. Yue, J. Wang, W. Li, M. Sun, C. Gu, L. Zeng, LINC00668 promotes tumorigenesis and progression through sponging miR-188-5p and regulating USP47 in colorectal cancer, *Eur J Pharmacol* **858**, 172464 (2019).
39. L. Yu, L. Dong, Y. Wang, L. Liu, H. Long, H. Li, J. Li, X. Yang, Z. Liu, G. Duan, X. Dai, Z. Lin, Reversible regulation of SATB1 ubiquitination by USP47 and SMURF2 mediates colon cancer cell proliferation and tumor progression, *Cancer Lett* **448**, 40–51 (2019).
40. S.-H. Kao, H.-T. Wu, K.-J. Wu, Ubiquitination by HUWE1 in tumorigenesis and beyond, *Journal of Biomedical Science* **25**, 67 (2018).
41. R. Buj, K. M. Aird, p16: cycling off the beaten path, *Mol Cell Oncol* **6** (2019), doi:10.1080/23723556.2019.1677140.

Figures

Figure 1

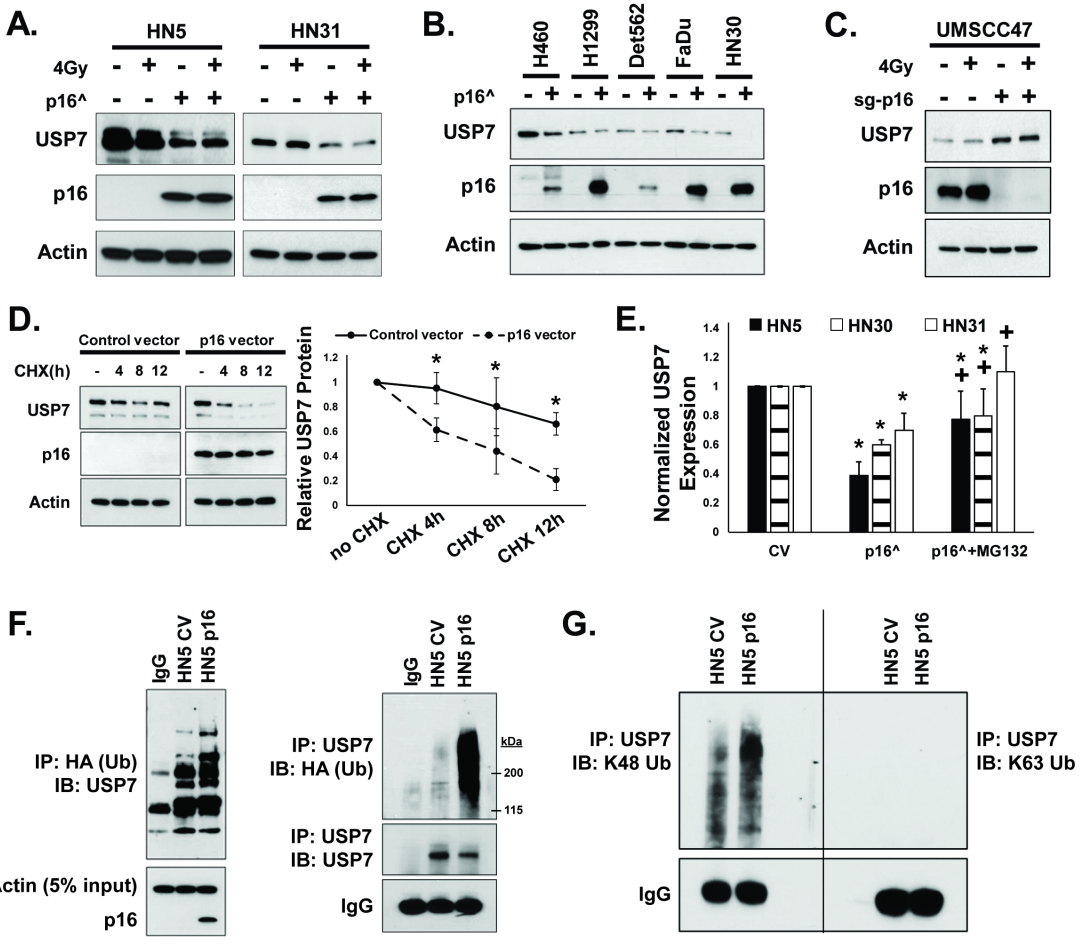

Figure 1

p16 inhibits USP7 levels by increasing its ubiquitination and degradation. A) Immunoblot of indicated proteins following the combination of radiation and forced expression of control vector or p16 in HN5 and HN31 HPV (-) HNSCC cell lines. B) Immunoblot following forced expression of control vector or p16 in in multiple HPV (-) HNSCC and NSCLC cell types. C) Immunoblot following CRISPR KO of p16 in an HPV (+) cell line (UM-SCC-47). D) Cyclohexamide chase assay in HN-5 (HPV (-)/p16 (-)) cells expressing

exogenous control vector or p16. E) MG132 rescue experiment in several HPV (-)/p16 (-) cell types (HN5, HN30 and HN31) following forced expression of p16 or control vector. Data are densitometry from immunoblots shown in Supplemental Fig. 2C and presented as mean ± SEM. F) HN5 cells expressing HA-tagged ubiquitin (Ub) and either control vector or p16 were analyzed via immunoprecipitation (IP) of HA and immunoblot of USP7 (left) or IP of USP7 and immunoblot of HA (right). G) HN5 cells expressing either control vector or p16 were analyzed via IP of USP7 followed by immunoblot for either K48- (left) or K63- (right) linked ubiquitin. * - p<0.05 versus control; + - p<0.05 vs. p16 forced expression.

Figure 2

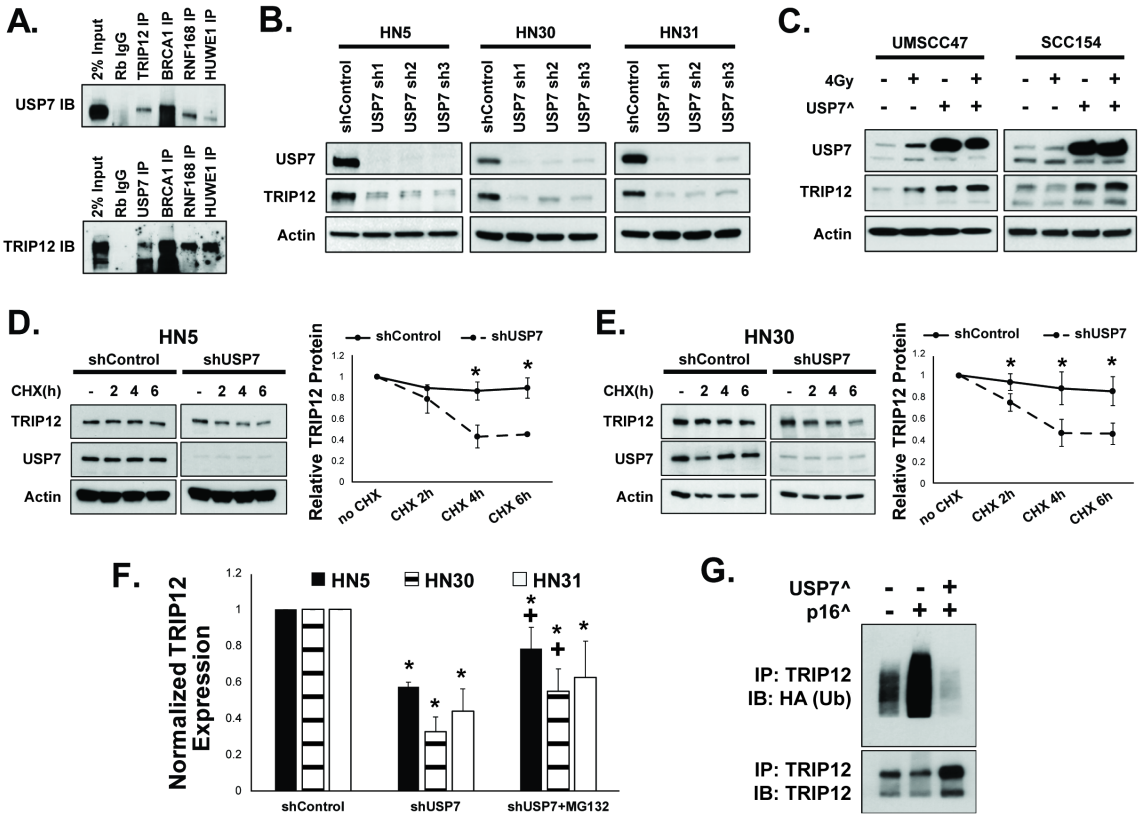

Figure 2

USP7 stabilizes TRIP12 via deubiquitination. A) IP for the indicated proteins in HPV (-) HN5 cells followed by immunoblot for either USP7 (top) or TRIP12 (bottom). B & C) Immunoblot of USP7 and TRIP12 in representative HPV (-)/p16 (-) cells stably expressing control or multiple shRNAs to USP7 (B) or representative HPV (+)/p16 (+) cells expressing control vector or USP7 (C). D & E) Cyclohexamide chase experiments in HN5 (D) and HN30 (E) HPV (-)/p16 (-) cells expressing control or shRNA for USP7 (shUSP7). F) MG132 rescue experiment in several HPV (-)/p16 (-) cell types (HN5, HN30 and HN31) expressing control or shUSP7. Data are densitometry from immunoblots shown in Supplemental Fig. 3C and presented as mean ± SEM. G) IP for TRIP12 and immunoblot for HA or TRIP12 in HN5 cells expressing Ub-tagged HA and either: control vector, p16 alone or USP7 and p16. * - $p<0.05$ versus control; + - $p<0.05$ vs. shUSP7.

Figure 3

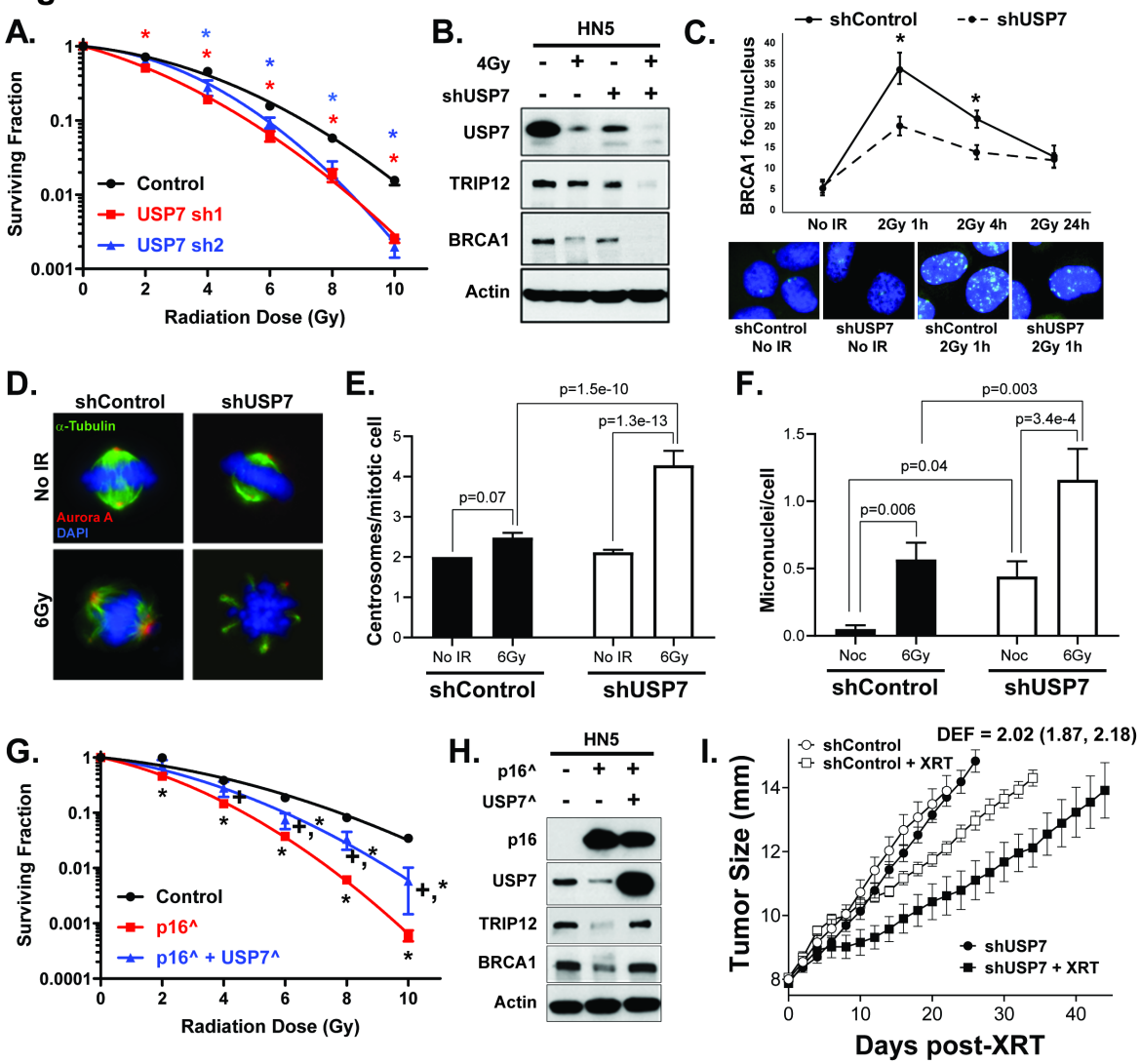

Figure 3

p16 inhibits USP7 leading to increased radiosensitivity. A-C) Clonogenic survival assay (A), immunoblot (B) and BRCA1 foci (representative images below the compiled averages) (C) in HN5 cells stably expressing control or shUSP7 constructs. D) Representative images in the indicated groups (green=α-Tubulin, red=Aurora A kinase, blue=DAPI). E & F) Centrosomes/mitotic cells (E) and micronuclei/cells (F) in HN5 cells stably expressing control or shUSP7 constructs. G & H) Clonogenic survival assay (G) and

immunoblot (H) in HN5 cells stably expressing control vector, p16 or p16 and USP7. I) In vivo tumor growth delay following intramuscular injection of HN5 cells expressing control or shUSP7 and treatment with 4 Gy x 5 days (20 Gy total). Composite data are presented as mean ± SEM. * - p<0.05 versus control; + - p<0.05 vs. p16 forced expression.

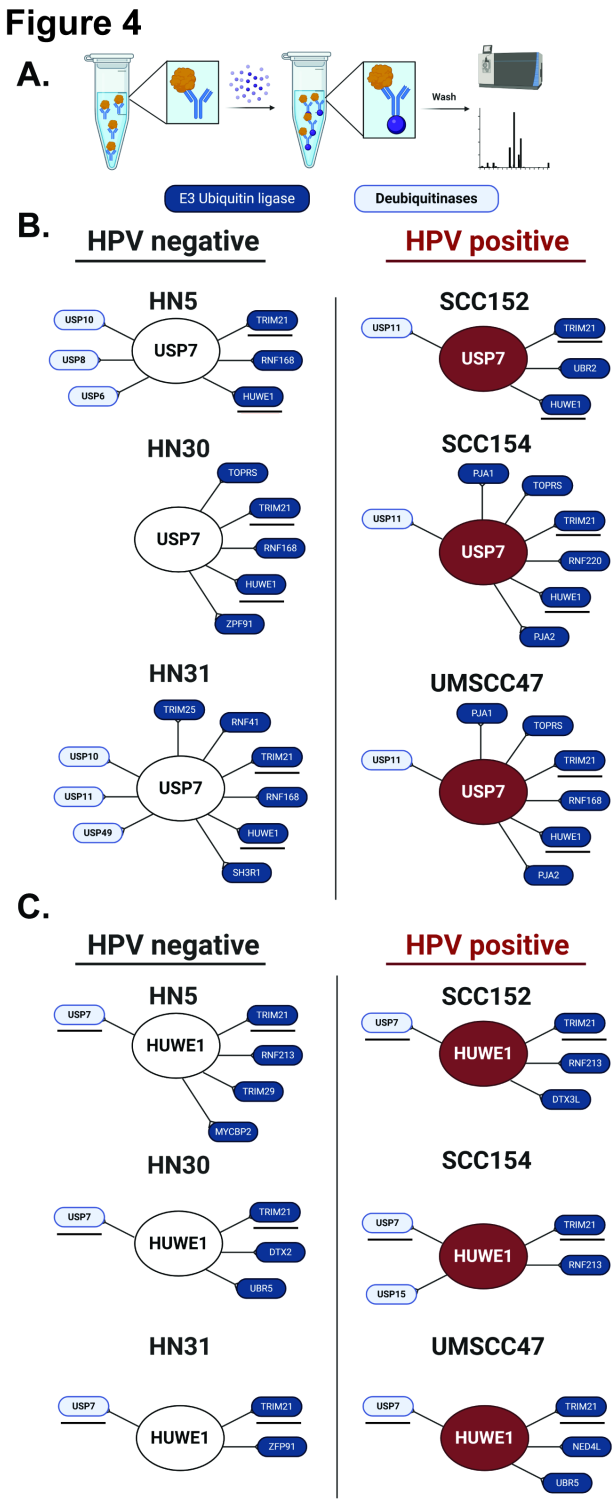

Figure 4

IP/MS identifies TRIM21 and HUWE1 as common E3 ubiquitin ligases for USP7. A) Basic schema for the experiment, with lysate incubated with either USP7 or HUWE1 antibody, followed by incubation with Protein-A Sepharose beads. The beads were then washed, centrifuged and analyzed via mass spectrometry. B & C) E3 ubiquitin ligases (dark blue) and deubiquitinases identified by IP/MS following IP for either USP7 (B) or HUWE1 (C) in HPV (+) and HPV (-) cells are shown. Targets common to all cell lines examined are underlined in black.

Figure 5

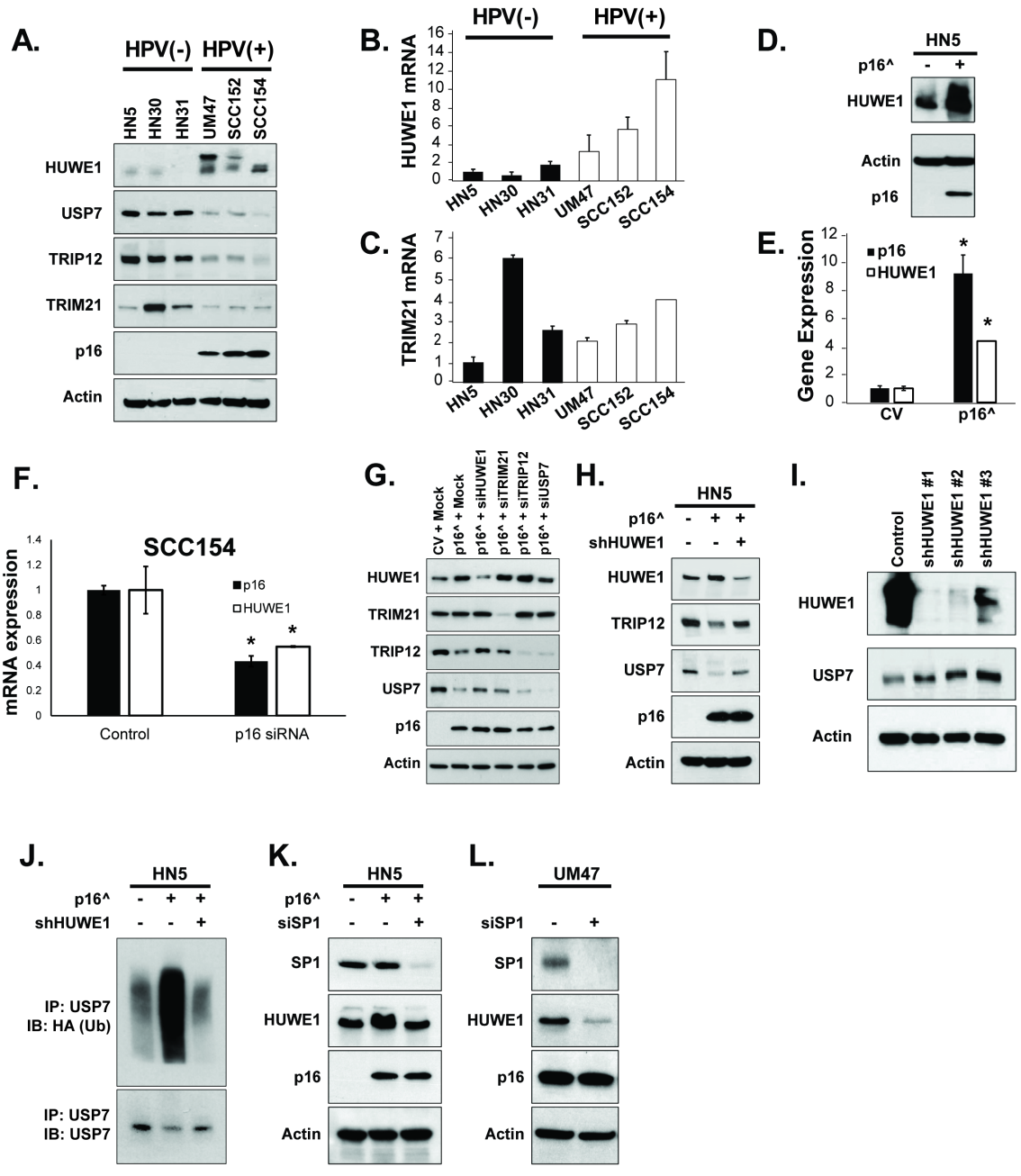

Figure 5

p16 represses USP7 via transcriptional activation of HUWE1. A-C) Immunoblot (A) and RT-PCR for HUWE1 (B) and TRIM21 (C) in HNSCC cell lines with indicated HPV status. D & E) Immunoblot (D) and RT-PCR (E) for the indicated genes in HN5 cells expressing control vector or p16. F) RT-PCR for the indicated genes in UM-SCC-47 HPV (+) cells transfected with siRNA targeting p16. G & H) Immunoblot in HN5 HPV (-) cells expressing control vector or p16 and siRNA for the indicated genes (G) or stably expressed control or HUWE1 shRNA (shHUWE1) (H). I) Immunoblot in SCC-154 cells stably expressing control or shRNA to HUWE1. J) IP for USP7 and immunoblot for HA in HN5 cells expressing HA-tagged Ub and either: control vector, p16 or p16 and shHUWE1. K) Immunoblot in HN5 cells expressing either control vector, p16 or p16 and siRNA to SP1 (siSP1). L) Immunoblot in UM-SCC-47 cells expressing control or siSP1. Composite data are presented as mean ± SEM. * - $p<0.05$ versus control for indicated gene.

Figure 6

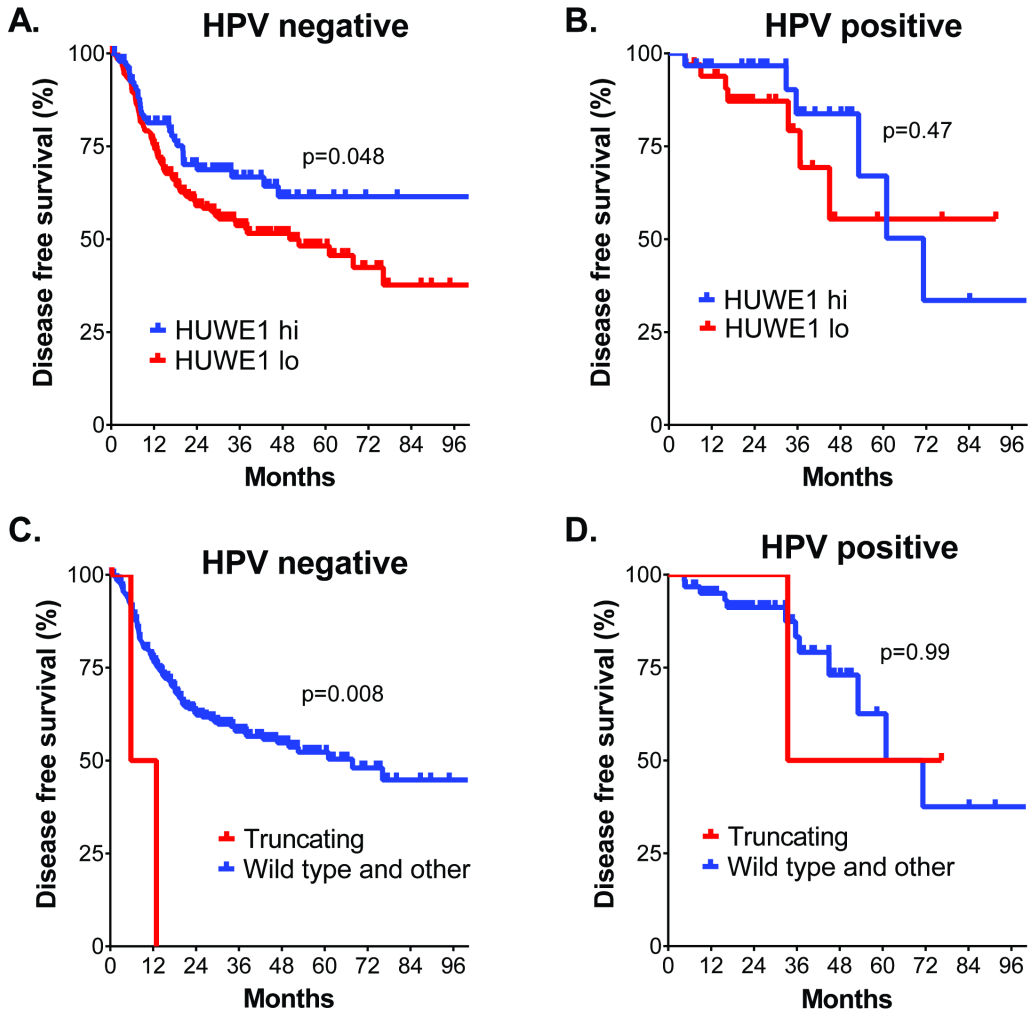

Figure 6

Decreased HUWE1 expression is associated with worse disease-free survival in HPV (-) HNSCC. Patients from the Head and Neck TCGA cohort were divided into groups based upon HPV status, HUWE1 mRNA expression (uppermost tertile (hi, blue line) vs. lower two tertiles (lo, red line)) and mutation status (truncating (red line) vs. other/wild type (blue line)), and DFS was analyzed using log rank statistics, with p-values shown.

Figure 7

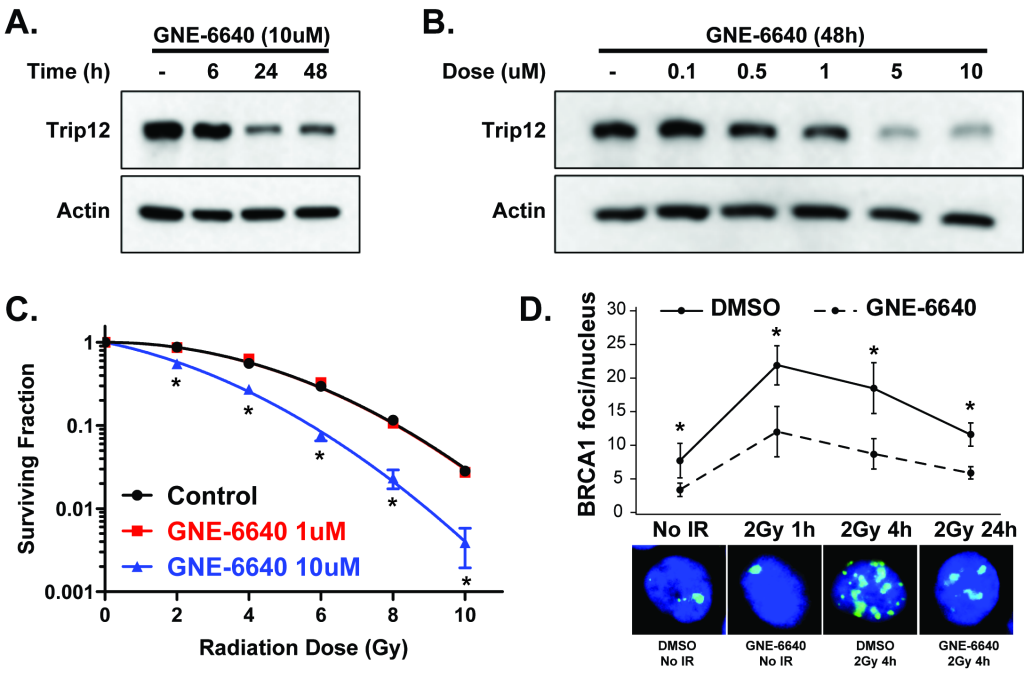

Figure 7

USP7 is a druggable target to increase radiosensitivity. A-D) Immunoblot (A & B), clonogenic survival (C) and BRCA1 foci formation (D) in HN5 cells treated with the USP7 inhibitor GNE-6640. Composite data are presented as mean ± SEM. * - $p<0.05$ versus control.

Figure 8

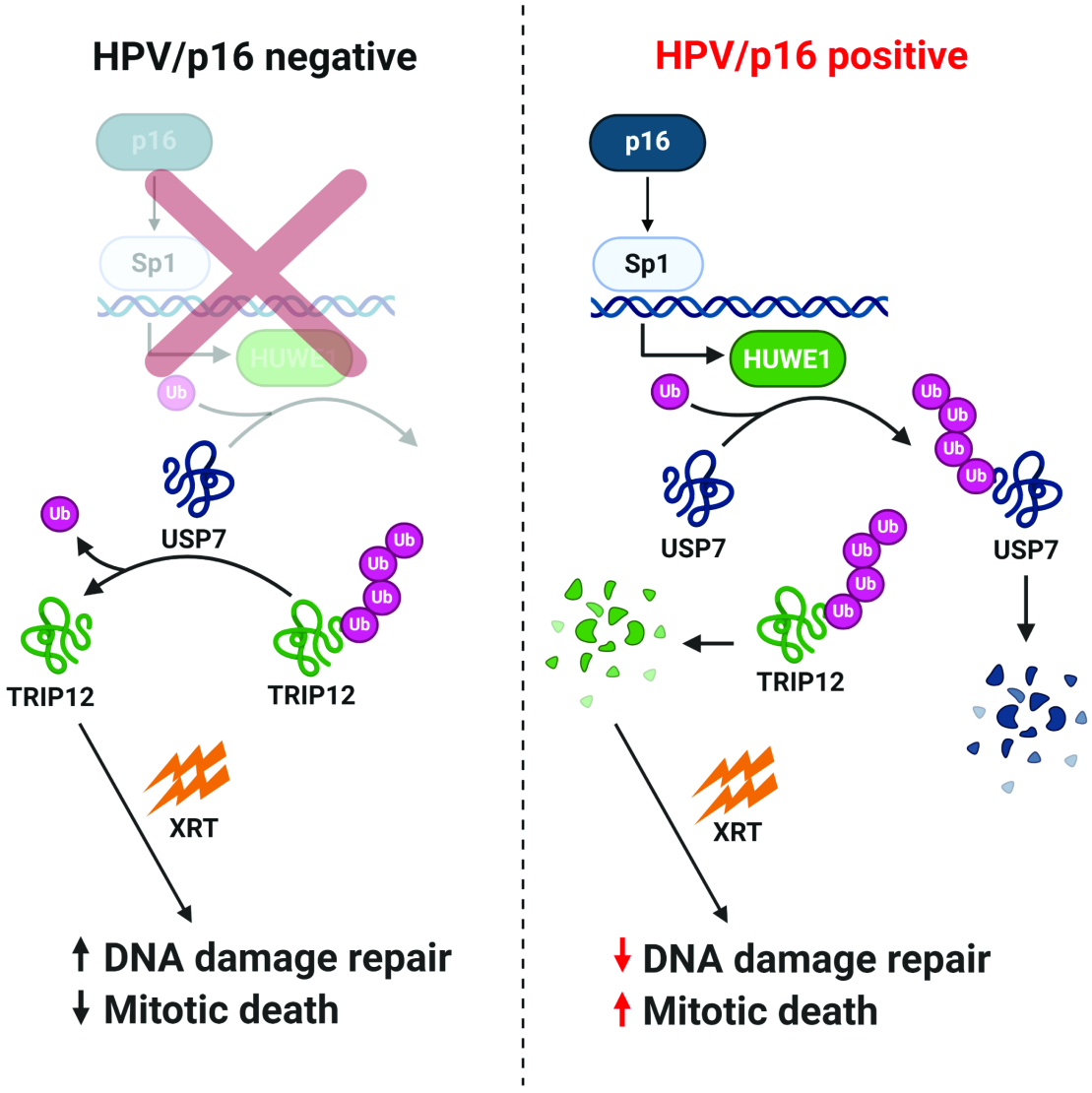

Figure 8

Potential pathway linking p16 to DNA damage repair via ubiquitin signaling.

Supplementary Files

This is a list of supplementary files associated with this preprint. Click to download.

- Supplementaltableandfigures3.29.21.docx